

## Stochastic resonance in the strong-forcing limit

L. Gammaitoni,<sup>1</sup> F. Marchesoni,<sup>1,2</sup> E. Menichella-Saetta,<sup>3</sup> and S. Santucci<sup>3</sup>

<sup>1</sup>Istituto Nazionale di Fisica Nucleare, Sezione di Perugia, I-06100 Perugia, Italy

<sup>2</sup>Dipartimento di Matematica e Fisica, Università di Camerino, I-62032 Camerino, Italy

<sup>3</sup>Dipartimento di Fisica, Università di Perugia, I-06100 Perugia, Italy

(Received 5 January 1995)

A recent theory [V. A. Shneidman, P. Jung, and P. Hänggi, Phys. Rev. Lett. **72**, 2682 (1994)] for periodically driven bistable systems in the limit of weak noise is assessed by means of analog simulation in the case of strong forcing. Two structures of dips and peaks for even multiples of the forcing frequency become detectable *simultaneously* in the relevant spectral density by decreasing the noise intensity. Stochastic resonance in such a system is also investigated.

PACS number(s): 05.40.+j

Stochastic resonance (SR) was predicted originally [1] for a simple symmetric bistable process  $x(t)$  driven by both a random noise, white and Gaussian, and an external sinusoidal bias and detected, later, in a variety of more complicated systems [2]. SR can be equivalently interpreted as either a resonant amplification of the amplitude  $\langle x \rangle$  of the periodic component of  $x(t)$  (conventional SR) [3–7], or a resonant synchronization of the switching mechanism of the bistable process with the periodic bias [4,8,9]. In particular, on keeping the forcing amplitude  $A$  and frequency  $\omega_0 = 2\pi\nu_0$  fixed,  $\langle x \rangle$  grows sharply with the noise intensity  $D$  until it reaches a maximum and, then, decreases slowly according to a certain power law. At variance with the notion of ordinary resonance,  $\langle x \rangle$  is a monotonically decreasing function of  $\omega_0$ . The representation of SR as a *bona fide* resonance [8] is well illustrated by mapping the continuous stochastic process  $x(t)$  into a stochastic point process  $t_i$  [4,9]. If  $t_i$  denotes the sequence of  $x(t)$  switching times (suitably defined by introducing symmetric crossing levels [9]), the quantities  $T(i) = t_i - t_{i-1}$  represent the residence times between two subsequent switching events. The normalized distributions of the residence times,  $N(T)$ , exhibit a structure of peaks centered at  $T_n = (n - \frac{1}{2})T_0$ , for  $n = 1, 2, \dots$ , with exponentially decreasing amplitude and finite size [4,10], superimposed on an exponentially decaying background (see, e.g., Fig. 1). [4,11] SR occurs when the synchronization effect is maximum, i.e., when, by tuning either  $D$  or  $\omega_0$ , the first peak of  $N(T)$  is made dominant over both the background and the remaining peaks [8].

In a recent paper [12], Shneidman, Jung, and Hänggi (SJH) investigated a bistable process  $x(t)$  in the limit  $Ax_m/D \rightarrow \infty$ . For small noise intensities, i.e., for  $D$  smaller than its SR value (in both the conventional and synchronization-based interpretation),  $N(T)$  exhibits a pronounced peak structure (Fig. 1) and, consequently, the subtracted spectral density  $\tilde{S}(\omega)$  (defined by subtracting all  $\delta$ -like terms corresponding to the periodic components of the relevant correlation function) develops a series of dips centered at  $2n\omega_0$ , according to the approximate law

$$\tilde{S}(\omega) = \frac{x_m^2 \mu(1-\mu)}{\omega^2 \Delta(1+\mu)} \frac{1 - \cos(\omega\Delta)}{[1 - \mu \cos(\omega\Delta)]^2 + \mu^2 \sin^2(\omega\Delta)}, \quad (1)$$

where  $\Delta$  coincides with the half forcing period, i.e.,  $\Delta = T_0/2$  and  $T_0 = 2\pi/\omega_0$ . Here,  $\pm x_m$  denote the stable values of the unbiased bistable process and  $\mu$  is the key parameter of SJH theory discussed below. Equation (1) is a universal law, since it only reproduces the *interwell* dynamics of the process, independently of the exact form of the relevant bistable drift term. Furthermore, its validity is restricted to values of the forcing frequency larger than  $\omega_K^{max}(D/Ax_m)^{1/2}$ , where  $\omega_K^{max}$  is the maximal switching rate in the presence of bias [12].

The *intrawell* dynamics (with restoring constant  $\omega_r$ ) is modulated by the periodic excursions that the stable values of  $x(t)$  perform around  $\pm x_m$ , respectively, when subjected to the periodic bias. Due to the  $x \rightarrow -x$  symmetry of the unbiased process, this effect may originate a series of peaks at  $2n\omega_0$  in the subtracted spectral density. For large  $\omega_0$  values, i.e.,  $\omega_0 \gg (D/Ax_m)^{1/2}(\omega_r x_m/A)\omega_K^{max}$ , such peaks are expected to supersede the dips predicted in Eq. (1) [12]. Their height and width strongly depend on the exact form of the bistable drift term of the process under study.

In the present work we assessed the predictions of SJH theory by means of an analog simulation [13]. In particular,

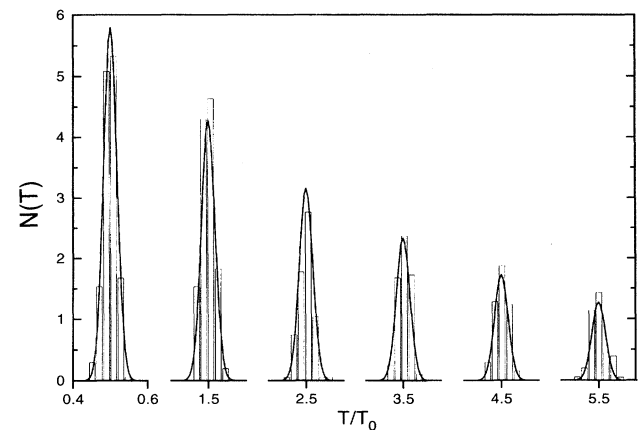


FIG. 1. Residence time distribution for  $\nu_0 = 41$  Hz. Parameter values are as follows:  $\Delta V/D = 1.6 \times 10^3$ ,  $Ax_m/D = 2.3 \times 10^3$ , and  $a = 3.2 \times 10^4 \text{ sec}^{-1}$  (estimated error 5%). The solid line represents the fitting law of Ref. [18] with  $\delta T_p/T_0 = 1.8 \times 10^{-2}$  and  $\delta\omega_d/\omega_0 = 0.3$ .

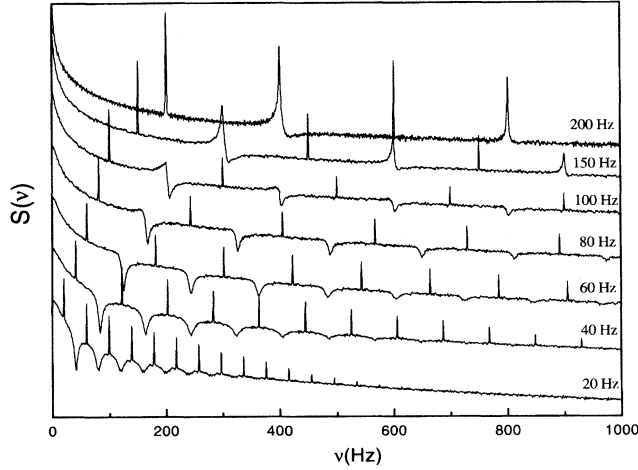


FIG. 2. Spectral densities (arbitrary units) of the full signal for different values of  $\nu_0$ . Other circuital parameters are as in Fig. 1.

we produced evidence of the simultaneous existence of both dips and peaks in the spectral density of a periodically driven bistable process with  $Ax_m/D \rightarrow \infty$ .

As in Ref. [12] we focused our attention on the quartic bistable process

$$\dot{x} = -V'(x) + \xi(t) + A \cos(\omega_0 t), \quad (2)$$

where  $V(x) = -ax^2/2 + bx^4/4$ ,  $\omega_r = 2a$ , and  $\pm x_m$  coincide with the minima of  $V(x)$  and are separated by the barrier  $\Delta V = a^2/4b$ . Our noise generator produces a random signal  $\xi(t)$  with zero mean value, Gaussian distribution, and correlation function

$$\langle \xi(t)\xi(0) \rangle = (D/\tau) \exp(-|t|/\tau). \quad (3)$$

Here,  $\tau$  is taken so small ( $a\tau = 0.15$ ) that the right-hand side (rhs) term of Eq. (3) approximates a  $\delta$  function. In order to explore the entire frequency interval studied by SJH, we employed a spectrum analyzer (model CF6400, manufactured by Ono-Sokki, Japan) with dynamical range of up to 145 dB. Furthermore, we restricted ourselves to the *strong-forcing limit*

$$0 \ll A/A_c < 1, \quad (4)$$

where  $A_c x_m = 8\Delta V/3\sqrt{3}$ . Here  $A_c$  stands for the critical value of the forcing amplitude above which the bistable nature of the process (2) would be lost. The weak-noise limit [12] was taken by selecting conveniently small  $D$  values, so that  $Ax_m/D$  ratios of the order of  $10^3$  were easily simulated.

The results of our simulation work can be summarized as follows.

(i) We separated the inter- and intrawell dynamics by filtering  $x(t)$  through a two-state ( $x = \pm 1$ ) filter and comparing the statistics of the filtered signal with that of the full signal, without changing the remaining circuital parameters. The nonsubtracted spectral densities  $S(\omega)$  for the full and the filtered signal are displayed in Figs. 2 and 3, respectively (see also Fig. 4). In both cases the number  $m$  of dips is larger than previously observed [14,15] and bounded from above according to the SJH inequality

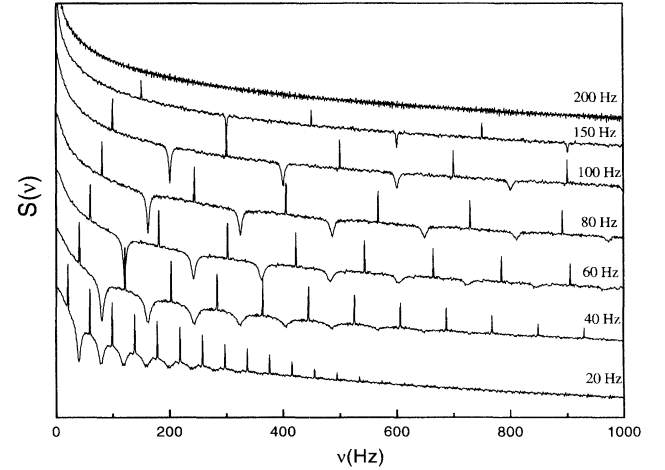


FIG. 3. Spectral densities (arbitrary units) of the filtered signal for different values of  $\nu_0$ . Other circuital parameters are as in Fig. 1.

$$m < \frac{1}{2} \left( \frac{Ax_m}{D} \right)^{1/2}. \quad (5)$$

(ii) The profile of all  $S(\omega)$  decays like  $\omega^{-2}$  as predicted in Ref. [12]. Deviations from such a universal behavior were observed in the spectral density of the full signal for  $\omega_0$  of the order of  $a$ . This means that the high frequency components of  $S(\omega)$  are filtered out by the intrawell relaxation dynamics with rate constant  $\omega_r$ . The validity of the power-law decay of Eq. (1) is thus extended well beyond the limiting value  $\omega_0(Ax_m/D)^{1/2}$  assumed rather conservatively by SJH [16].

(iii) The dip structure of  $S(\omega)$  becomes apparent by filtering  $x(t)$ , as implied by the approach of Ref. [12]. We verified that, within the accuracy of our statistical analysis, the dips are centered at  $2n\omega_0$ , their width  $\delta\omega_d$  is of the order of  $\omega_K^{max}(D/Ax_m)^{1/2}$  [17], insensitive to the dip index  $n$  and the forcing frequency  $\omega_0$ . Most notably, the dips tend to

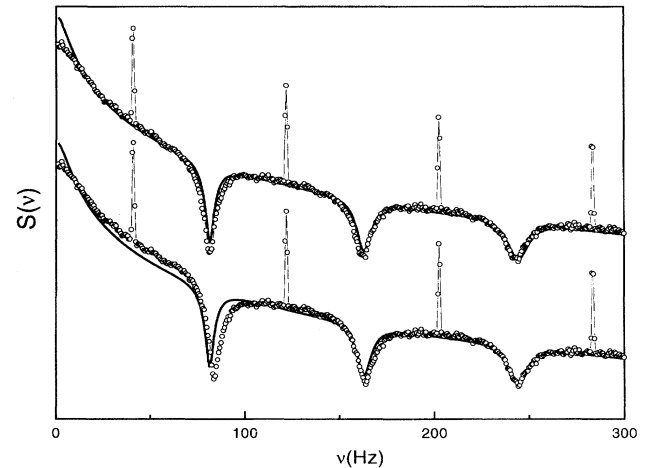


FIG. 4. Magnification of the curves of Figs. 2 (lower curve) and 3 (upper curve) for  $\nu_0 = 41$  Hz. The solid lines represent our theoretical prediction for  $S(\nu)$  based on Eq. (1).  $\delta T_p$  and  $\delta\omega_d$  are as in Fig. 1.

disappear with increasing  $\omega_0$  larger than  $\omega_K^{max}$  and their shape is not as sharp as predicted by Eq. (1), where  $S(\omega = 2n\omega_0) = 0$ .

(iv) No peak structure was observable in the subtracted spectral densities for the filtered signal, whereas for the full signal, broad peaks located in the vicinity to  $2n\omega_0$  were detected at relatively high values of the forcing frequency, namely, for  $\omega_0 \gtrsim \omega_K^{max}$ . Moreover, such peaks get sharper (i.e., higher and narrower) on further increasing  $\omega_0$ , and their height decreases with the peak index according to a power law. We checked that these properties strongly depend on the actual shape of the potential  $V(x)$ .

(v) Dips and peaks of  $S(\omega)$  may coexist for the full signal (Fig. 2). This happens for  $\omega_0 \sim \omega_K^{max}$ , as suggested in (iii) and (iv). In such a case, their position deviates slightly from the predicted value  $2n\omega_0$  by shifting respectively to the right and, possibly, to the left. This observation, which could not be reproduced analytically under the SJH approximations, confirms the results of some numerical computations by the same authors [see Fig. 1 (inset) of Ref. [12]]. The relative weight of dips and peaks depends markedly on the forcing frequency. At very low  $\omega_0$  values no peak is detectable and the curves of Figs. 2 and 3 approach one another. At high  $\omega_0$  values peaks dominate over dips, which, in turn, tend to vanish.

(vi) According to SJH theory, marked dip structures in  $S(\omega)$  correspond to multi-peaked residence time distributions. We checked that in the limit of weak noise and strong forcing, the shape of the  $n$ th  $N(T)$  peak is well approximated by a Gaussian function with standard deviation  $\delta T_p$  independent of  $n$ . The peak height  $N(T_n)$  decays according to the exponential law  $N(T_n) = N(T_1) \exp[-(n-1)\delta\omega_d/\omega_0]$  with  $\delta\omega_d$  defined in (iii) [18]. The two quantities  $\delta T_p$  and  $\delta\omega_d$  are apparently related by a phenomenological law of the type  $2D/\delta\nu_d \approx Ax_m \delta T_p / 2\pi$ , whence  $\delta\nu_d \delta T_p \approx 4\pi D / Ax_m$ .

On concluding, we discuss now the role of the key parameter  $\mu$  [12]

$$(1 - \mu)\omega_0 \equiv \omega_K^{max}(D/Ax_m)^{1/2} \quad (6)$$

introduced in Eq. (1). We recall that the characteristic frequency on the rhs of Eq. (6) appears in the present work as (a) the width  $\delta\omega_d$  of the  $S(\omega)$  dips (at least in the absence of peaks due to the intrawell dynamics), (b) the lower  $\omega_0$  bound for the existence of such dips, and (c) the exponential decay constant of the function  $N(T_n)$ , see (vi). In the strong-forcing regime (4) it is possible to discriminate between two clear-cut limiting values of the Kramers switching rate [10]. For  $t=0$  and  $A < A_c$ , the time-dependent potential  $V(x,t) \equiv V(x) - Ax \cos(\omega_0 t)$  in Eq. (2) exhibits two asymmetric wells: a shallower one on the left-hand side with maximal Kramers rate  $\omega_K^{max}$  and a deeper one on the rhs with

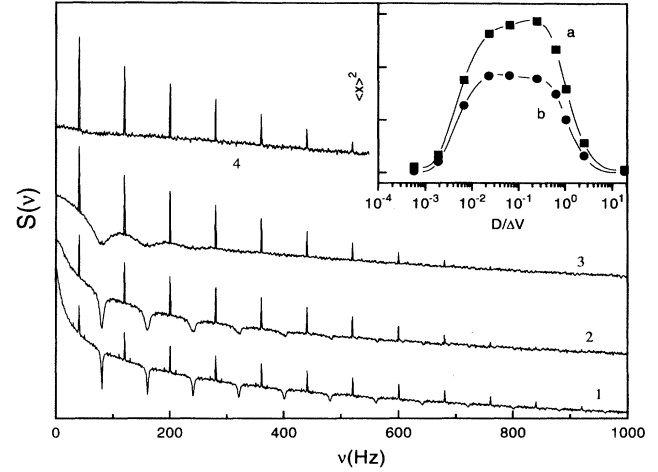


FIG. 5. Spectral densities (arbitrary units) of the filtered signal for different values of  $D$ :  $D/\Delta V = 5.6 \times 10^{-4}$  (curve 1),  $2.0 \times 10^{-3}$  (curve 2),  $7.0 \times 10^{-3}$  (curve 3), and  $2.3 \times 10^{-2}$  (curve 4). Inset:  $\langle x \rangle^2$  (arbitrary units) versus  $D$  for the full (curve a) and the filtered (curve b) signal. All remaining parameters are as in Fig. 1.

minimal rate  $\omega_K^{min}$ . In the weak-noise limit,  $\omega_K^{min} \ll \omega_K^{max}$ . In the adiabatic approximation [19] it is possible to introduce *two time-dependent* switching rates  $r(t)$  (out of either potential well), which oscillate between  $\omega_K^{min}$  and  $\omega_K^{max}$  with period  $T_0$ . We verified that a SR behavior is detectable in the strong-forcing regime, too, by plotting  $\langle x \rangle^2$  versus  $D$  in Fig. 5 for both the full and the filtered signal. The amplitude of the periodic component of  $x(t)$  reaches its maximum for a small value of the noise intensity,  $D_{min}$ , roughly corresponding to the condition  $\omega_0 \sim \omega_K^{max}(D_{min})$ , and contrary to conventional SR, continues almost unchanged for a wide  $D$  range with upper bound,  $D_{max}$ , approximated by  $\omega_0 \sim \omega_K^{min}(D_{max})$ .

Finally, the actual shape of the  $S(\omega)$  dips can be determined more accurately than in Ref. [12]. Since the quantity  $2\Delta$  in Eq. (1) is a random variable with mean value  $T_0$  and *finite* standard deviation  $\delta T_p$ , it seems quite natural to take the average of Eq. (1) with respect to  $\Delta$  rather than just imposing  $\Delta = T_0/2$ . Furthermore, our analysis of the  $N(T)$  peak profile (Fig. 1) suggests that  $\Delta$  is distributed according to a Gaussian function with the appropriate mean value and standard deviation reported in (vi). In Fig. 4 we compare the theoretical curve for  $S(\omega)$  thus obtained with the results of analog simulation. The agreement is particularly close in the case of the filtered signal. Most notably, the finite depth of the  $S(\omega)$  dips is correctly reproduced as a result of the averaging procedure, with no relevant change in the dip width.

[1] R. Benzi, G. Parisi, A. Sutera, and A. Vulpiani, *Tellus* **34**, 10 (1982).

[2] See, for example, Proceedings of the NATO Workshop on Stochastic Resonance in Physics and Biology, edited by F. Moss,

A. Bulsara, and M. F. Shlesinger [*J. Stat. Phys.* **70**, 1 (1993)].

[3] B. McNamara and K. Wiesenfeld, *Phys. Rev. A* **39**, 4854 (1989).

[4] L. Gammaitoni, F. Marchesoni, E. Menichella-Saetta, and S.

- Santucci, Phys. Rev. Lett. **62**, 349 (1989).
- [5] C. Presilla, F. Marchesoni, and L. Gammaitoni, Phys. Rev. A **40**, 2105 (1989).
- [6] G. Hu, G. Nicolis, and C. Nicolis, Phys. Rev. A **42**, 2030 (1990).
- [7] P. Jung and P. Hänggi, Europhys. Lett. **8**, 505 (1989).
- [8] L. Gammaitoni, F. Marchesoni, and S. Santucci, Phys. Rev. Lett. **74**, 1052 (1995).
- [9] L. Gammaitoni, F. Marchesoni, E. Menichella-Saetta, and S. Santucci, Phys. Rev. Lett. **71**, 3625 (1993).
- [10] T. Zhou, F. Moss, and P. Jung, Phys. Rev. A **42**, 3161 (1990).
- [11] A. Simon and A. Libchaber, Phys. Rev. Lett. **68**, 3375 (1992).
- [12] V. A. Shneidman, P. Jung, and P. Hänggi, Phys. Rev. Lett. **72**, 2682 (1994); Europhys. Lett. **26**, 571 (1994).
- [13] F. Marchesoni, E. Menichella-Saetta, M. Pochini, and S. Santucci, Phys. Rev. A **37**, 3058 (1987).
- [14] T. Zhou and F. Moss, Phys. Rev. A **41**, 4255 (1990).
- [15] L. Kiss, Z. Gingl, Z. Marton, J. Kertesz, F. Moss, G. Schmera, and A. Bulsara, J. Stat. Phys. **70**, 451 (1993).
- [16] A further deviation from the  $\omega_0^{-2}$  decay law of  $S(\omega)$  for both signals becomes detectable at finite noise correlation times, i.e., for  $\omega_0\tau \gtrsim 1$ .
- [17] Our experimental determination of  $\omega_K^{max}$  is rather crude. For the circuital parameter values reported in Fig. 1  $\omega_K^{max} \sim 4 \times 10^3 \text{ sec}^{-1}$ .
- [18] It follows that  $N(T)$  may be fitted by the approximate law  $N(T) = [1 - \exp(-\delta\omega_d/\omega_0)] \sum_{n=1}^{\infty} \exp[-(n-1)\delta\omega_d/\omega_0] G(T-T_n)$ , where  $G(x)$  denotes a normalized Gaussian distribution with standard deviation  $\delta T_p$ .
- [19] The validity of the adiabatic approximation is restricted by the requirement that  $[[1/r(t)]^2 [d^2r(t)/dt^2]]|_{t=0} \gg r(0)$  with  $r(0) = \omega_K^{max}$ . On making use of the Kramers formula for  $r$ , this inequality reduces to the condition  $\mu \rightarrow 1$  [12] and sets the intrinsic limit  $(\delta\omega_d/\omega_0)^2 \approx |r^3(0)/r''(0)|$  to the synchronization effect achievable in a continuous bistable system; see items (iii) and (vi).